Theory of phason drag effect on thermoelectricity

Hidetoshi Fukuyama●

Tokyo University of Science, Shinjuku, Tokyo 162-8601, Japan

Masao Ogata●*

Department of Physics, University of Tokyo, Bunkyo, Tokyo 113-0033, Japan

Lee, Rice, and Anderson, in their monumental paper [Solid State Commun. **14**, 703 (1974)], proved the existence of a collective mode describing the coupled motion of electron density and phonons in a one-dimensional incommensurate charge density wave in the Peierls state. This mode, which represents the coherent sliding motion of electrons and lattice distortions and affects low-energy transport properties, is described by the phase of the complex order parameter of the Peierls condensate, leading to Fröhlich superconductivity in pure systems. Once spatial disorder is present, however, the phason is pinned, and the system is transformed into an insulating ground state: a dramatic change. Since phasons can be considered an ultimate phonon drag effect, it is of interest to see its effects on thermoelectricity, which is studied in the present paper based on linear response theory of Kubo and Luttinger. The result indicates that a large absolute value of the Seebeck coefficient proportional to the square root of the resistivity is expected at low temperatures $k_B T/\Delta \ll 1$ (Δ is the Peierls gap) with a sign opposite to the electronic contributions in the absence of the Peierls gap.

I. INTRODUCTION

Various aspects of the thermoelectric effect have been extensively studied both theoretically and experimentally [1,2]. Especially, recent social needs reflecting the fact that quite a large fraction of primary energy is wasted as heat strongly urge the quest for materials with high thermoelectric capability. Motivated by this understanding, we have been developing studies toward the systematic understanding of thermoelectricity beyond Boltzmann transport theory based on the linear response theory of Kubo [3] and Luttinger [4]. Those include the spin-Seebeck effect free from contamination of electric current [5], identification of the range of validity of the Sommerfeld-Bethe relation [6], the phonon drag effect in the presence of the impurity band [7], and n-type and bipolar carbon nanotubes, indicating the importance of band-edge engineering and the possible probing of morphology of samples in experiments [8,9]. In this paper phason drag effects are studied as an example of the phonon drag, which has long been known in doped semiconductors to play important roles [10–13] and was proposed very recently to be the case also in FeSb$_2$ [7].

A phason is the collective mode of electron-phonon coupled systems in the incommensurate Peierls phase resulting in a charge density wave (CDW), where spatially modulated electron density and lattice distortion are locked with the same periodicity. Lee, Rice, and Anderson (LRA) [14] discovered this phason in view of the experimental

finding of extraordinary conductivity in tetrathiofulvalinium tetracyanoquinodimethan (TTF-TCNQ), leading to the controversial discussions of possible Fröhlich superconductivity [15]. When the CDW moves, electrons and lattice distortion move together (sliding mode), and the dynamics is described by the phase of the complex order parameter of the Peierls phase, then called a phason. Hence, a phason is considered to be the ultimate form of phonon drag. In contrast to the case of superconductivity, a phason, which is due to diagonal long-range order, is sensitive to spatial inhomogeneity resulting in impurity pinning. Once a phason is pinned, there is no sliding, and the state is insulating at absolute zero. However, at finite temperature, a pinned phason will move locally by the creation of soliton pairs induced by the thermal excitation, leading to the activation-type temperature dependence of conductivity L_{11} [16]. In this paper we study thermoelectric conductivity L_{12} and the Seebeck coefficient $S = L_{12}/T L_{11}$, with T being temperature, due to phason drag in such a low-temperature region for the one-dimensional electron-phonon Peierls phase using the thermal Green's function.

Regarding phason contributions to L_{12}, Yoshimoto and Kurihara [17] studied the electronic contribution in clean systems without disorder. In this paper, we explore the phason drag contributions in the presence of impurity pinning.

In Sec. II, we introduce the one-dimensional electron-phonon system and the phason. The formulation by LRA [14] is modified in accordance with the present framework. In Sec. III, the electrical conductivity due to the phason is discussed, and in Sec. IV, results of the phason drag contribution to L_{12} and the resulting Seebeck coefficient are given. Section V is devoted to a summary.

*ogata@phys.s.u-tokyo.ac.jp

II. ONE-DIMENSIONAL ELECTRON-PHONON SYSTEM AND PHASON

We consider a one-dimensional electron-phonon system using the Fröhlich model H_0 to describe the Peierls transition in the presence of random distribution of impurities H', $H = H_0 + H'$, where H_0 and H' are given as follows:

$$
\begin{aligned}
H_0 = &\sum_{p,\sigma} \varepsilon_p c_{p,\sigma}^\dagger c_{p,\sigma} + \sum_q \hbar\omega_q b_q^\dagger b_q \\
&+ \frac{1}{\sqrt{L}} \sum_{p,q,\sigma} g_q c_{p+q,\sigma}^\dagger c_{p,\sigma}(b_q + b_{-q}^\dagger),
\end{aligned}
$$

$$
\begin{aligned}
H' &= \sum_i \int v(x - R_i)\rho(x)dx \\
&= \frac{1}{L} \sum_i \sum_{p,q,\sigma} e^{-iqR_i} v_q c_{p+q,\sigma}^\dagger c_{p,\sigma}. \quad (1)
\end{aligned}
$$

Here, $c_{p,\sigma}^\dagger$ and $b_q^\dagger$ are creation operators for a one-dimensional Bloch electron and a phonon with energies ε_p and $\hbar\omega_q$, respectively, L is the length of the system, g_q represents the electron-phonon coupling constant, R_i represents the position of impurities, $v(x)$ and $\rho(x)$ are the impurity potential and electron density, respectively, and v_q is the Fourier transform of $v(x)$. First, we focus on H_0, and the effects of H' will be treated later.

In the mean-field theory of the uniform Peierls phase, the lattice distortion is described by the order parameter

$$
\Delta = \frac{1}{\sqrt{L}} g_Q(\langle b_Q \rangle + \langle b_{-Q}^\dagger \rangle) \equiv e^{i\phi} \Delta_0 \quad (2)
$$

($\Delta_0 > 0$), with $Q = 2k_F$, and the mean-field Hamiltonian for electrons becomes

$$
H_{\mathrm{MF}} = \sum_{k,\sigma} \left(c_{\frac{Q}{2}+k,\sigma}^\dagger, \quad c_{-\frac{Q}{2}+k,\sigma}^\dagger \right) \begin{pmatrix} \xi_k & \Delta \\ \Delta^* & -\xi_k \end{pmatrix} \begin{pmatrix} c_{\frac{Q}{2}+k,\sigma} \\ c_{-\frac{Q}{2}+k,\sigma} \end{pmatrix}, \quad (3)
$$

where $|k| < Q/2$ and we have linearized the energy dispersion as $\varepsilon_p - \mu \sim \xi_k$ in the vicinity of $k_F = Q/2$ with $\xi_k = \hbar v_F k$ and $k = p - k_F$. Similarly, in the vicinity of $-k_F = -Q/2$, we have linearized $\varepsilon_p - \mu \sim -\xi_k$ with $k = p + k_F$. It should be noted that we consider the cases where v_F is positive and negative. The self-consistency equation for Δ is

$$
\Delta = \frac{4g_Q^2}{\hbar\omega_Q L} \sum_k \frac{\Delta}{2E_k} \{f(-E_k) - f(E_k)\}, \quad (4)
$$

where

$$
E_k = \sqrt{\xi_k^2 + |\Delta|^2} \quad (5)
$$

and $f(\varepsilon) = 1/(e^{\beta\varepsilon} + 1)$ is the Fermi distribution function with $\beta = 1/k_B T$.

As performed by LRA, Δ can be chosen to be real (i.e., $\phi = 0$) in the uniform mean-field solution by redefining the operator as $\tilde{c}_{\frac{Q}{2}+k,\sigma}^\dagger = c_{\frac{Q}{2}+k,\sigma}^\dagger e^{i\phi}$, while $c_{-\frac{Q}{2}+k,\sigma}^\dagger$ is not changed. However, we keep ϕ in the following since ϕ is no longer uniform in the presence of impurity pinning and the dynamics of the phason is represented by the spatial and temporary

dependence of ϕ as described in the phase Hamiltonian [18]. In fact, the charge density is given as

$$
\rho(x,t) = n_e + \rho_0 \cos[Qx + \phi(x,t)], \quad (6)
$$

where n_e is the average electron density, $\rho_0 = \hbar\omega_Q|\Delta|/2g_Q^2$, and $\partial\phi(x,t)/\partial t$ and $\partial\phi(x,t)/\partial x$ give the electric current density and the local modulation of electric charge density, respectively [19,20].

To study the phason mode and amplitude mode in the case of a constant ϕ, we introduce phonon propagators in the matrix form

$$
\begin{aligned}
\mathcal{D}_{mn}(q, \tau) = -\langle T_\tau \{ &[b_{mQ+q}(\tau) + b_{-mQ-q}^\dagger(\tau)] \\
&\times [b_{nQ+q}^\dagger(0) + b_{-nQ-q}(0)] \} \rangle, \quad (7)
\end{aligned}
$$

where $m, n = \pm$, and electron Green's functions

$$
\mathcal{G}_{mn}(k, \tau) = -\langle T_\tau [c_{mQ/2+k,\sigma}(\tau) c_{nQ/2+k,\sigma}^\dagger(0)] \rangle. \quad (8)
$$

For the mean-field Hamiltonian of Eq. (3), the Fourier transform of $\mathcal{G}_{mn}(k, \tau)$ is given by

$$
\mathcal{G}(k, i\varepsilon_n) = \frac{1}{(i\varepsilon_n)^2 - E_k^2} \begin{pmatrix} i\varepsilon_n + \xi_k & \Delta \\ \Delta^* & i\varepsilon_n - \xi_k \end{pmatrix}, \quad (9)
$$

where $\varepsilon_n = (2n + 1)\pi k_B T$ is the Matsubara frequency (n is an integer).

As shown by LRA, the Dyson equation for $\mathcal{D}_{mn}$ leads to

$$
\begin{aligned}
&\mathcal{D}_{++}(q, i\omega_\nu) \pm e^{-2i\phi} \mathcal{D}_{+-}(q, i\omega_\nu) \\
&= \frac{\mathcal{D}^{(0)}(i\omega_\nu)}{1 - [\Pi_{++}(q, i\omega_\nu) \pm e^{-2i\phi}\Pi_{+-}(q, i\omega_\nu)]\mathcal{D}^{(0)}(i\omega_\nu)}, \quad (10)
\end{aligned}
$$

where $\omega_\nu = 2\pi\nu k_B T$ is the Matsubara frequency (ν is an integer) and

$$
\begin{aligned}
&\Pi_{++}(q, i\omega_\nu) \\
&= 2g_Q^2 \frac{k_B T}{L} \sum_{k,n} \mathcal{G}_{++}(k+q, i\varepsilon_n + i\omega_\nu)\mathcal{G}_{--}(k, i\varepsilon_n),
\end{aligned}
$$

$$
\begin{aligned}
&\Pi_{+-}(q, i\omega_\nu) \\
&= 2g_Q^2 \frac{k_B T}{L} \sum_{k,n} \mathcal{G}_{+-}(k+q, i\varepsilon_n + i\omega_\nu)\mathcal{G}_{+-}(k, i\varepsilon_n), \quad (11)
\end{aligned}
$$

where $g_{Q+q} \sim g_Q$ has been assumed. [For completeness, the derivation of Eq. (10) is shown in Appendix A.] It is to be noted that the zeroth-order phonon propagator

$$
\mathcal{D}_{mn}^{(0)}(q, i\omega_\nu) = \delta_{mn} \frac{2\hbar\omega_{mQ+q}}{(i\omega_\nu)^2 - \hbar^2\omega_{mQ+q}^2} \quad (12)
$$

has been approximated as

$$
\mathcal{D}_{mn}^{(0)}(q, i\omega_\nu) \sim \delta_{mn} \mathcal{D}^{(0)}(i\omega_\nu) = \delta_{mn} \frac{2\hbar\omega_Q}{(i\omega_\nu)^2 - \hbar^2\omega_Q^2}. \quad (13)
$$

The denominator for $\mathcal{D}_{++} - e^{-2i\phi}\mathcal{D}_{+-}$ in Eq. (10) leads to a q-linear mode, $\omega = v|q|$ ($v > 0$), which is a phason, while that of $\mathcal{D}_{++} + e^{-2i\phi}\mathcal{D}_{+-}$ leads to the amplitude mode. Therefore, phason and amplitude propagators are defined as

$$
P(q, i\omega_\nu) = \mathcal{D}_{++}(q, i\omega_\nu) - e^{-2i\phi}\mathcal{D}_{+-}(q, i\omega_\nu),
$$

$$
A(q, i\omega_\nu) = \mathcal{D}_{++}(q, i\omega_\nu) + e^{-2i\phi}\mathcal{D}_{+-}(q, i\omega_\nu), \quad (14)
$$

respectively. For a small-q and small-$(i\omega_\nu)$ region, they become

$$P(q, i\omega_\nu) = \frac{2\hbar\omega_Q/(1+X)}{(i\omega_\nu)^2 - (\hbar v q)^2},$$

$$A(q, i\omega_\nu) = \frac{2\hbar\omega_Q/(1+X/3)}{(i\omega_\nu)^2 - \hbar^2\omega_{\rm am}^2(q)}, \quad (15)$$

where $X = \omega_Q g_Q^2/2\pi|v_{\rm F}|\Delta_0^2$, and the phason velocity v is given by

$$v = [X/(1+X)]^{1/2}|v_{\rm F}|. \quad (16)$$

The dispersion of the amplitude mode $\omega_{\rm am}(q)$ is

$$\omega_{\rm am}(q) = \sqrt{\frac{4X}{1+\frac{X}{3}}\Delta_0^2 + \frac{X}{3+X}(\hbar v_{\rm F}q)^2}. \quad (17)$$

The details of the calculations are shown in Appendix A.

III. ELECTRICAL CONDUCTIVITY DUE TO PHASONS

The Kubo formula for dynamical electrical conductivity for uniform electric field $\sigma(\omega)$ is given by

$$L_{11} = \frac{1}{i\omega}[\Phi_{11}(i\omega_\lambda \to \hbar\omega + i\delta) - \Phi_{11}(0)], \quad (18)$$

with

$$\Phi_{11}(i\omega_\lambda) = \frac{1}{L}\int_0^\beta d\tau \langle T_\tau[J_e(\tau)J_e(0)]\rangle e^{i\omega_\lambda\tau}. \quad (19)$$

Here, J_e is the electronic current,

$$J_e = -e\sum_{k,\sigma}\left(c_{\frac{Q}{2}+k,\sigma}^\dagger, \quad c_{-\frac{Q}{2}+k,\sigma}^\dagger\right)v_{\rm F}\sigma_z\begin{pmatrix}c_{\frac{Q}{2}+k,\sigma}\\ c_{-\frac{Q}{2}+k,\sigma}\end{pmatrix}, \quad (20)$$

where $-e$ is the electron charge ($e > 0$) and σ_z is the z component of Pauli matrices. As shown by LRA, the conductivity due to phasons is governed by processes in Fig. 1 [14]. For example, Fig. 1(a) gives the following contribution to $\Phi_{11}(i\omega_\lambda)$:

$$-g_Q^2\frac{4e^2v_{\rm F}^2(k_{\rm B}T)^2}{L^2}\sum_{k,k',\varepsilon_n,\varepsilon_n'}{\rm Tr}[\sigma_z\mathcal{G}(k,i\varepsilon_n+i\omega_\lambda)\sigma_+\mathcal{G}(k,i\varepsilon_n)]\mathcal{D}_{++}(0,i\omega_\lambda){\rm Tr}[\sigma_-\mathcal{G}(k',i\varepsilon_n'+i\omega_\lambda)\sigma_z\mathcal{G}(k',i\varepsilon_n')]$$

$$= -g_Q^2\frac{4e^2v_{\rm F}^2(k_{\rm B}T)^2}{L^2}\sum_{k,\varepsilon_n}\{\mathcal{G}_{++}(k,i\varepsilon_n+i\omega_\lambda)\mathcal{G}_{-+}(k,i\varepsilon_n) - \mathcal{G}_{-+}(k,i\varepsilon_n+i\omega_\lambda)\mathcal{G}_{--}(k,i\varepsilon_n)\}$$

$$\times\mathcal{D}_{++}(0,i\omega_\lambda)\sum_{k',\varepsilon_n'}\{\mathcal{G}_{++}(k',i\varepsilon_n'+i\omega_\lambda)\mathcal{G}_{+-}(k',i\varepsilon_n') - \mathcal{G}_{+-}(k',i\varepsilon_n'+i\omega_\lambda)\mathcal{G}_{--}(k',i\varepsilon_n')\}$$

$$= -g_Q^2\frac{4e^2v_{\rm F}^2(k_{\rm B}T)^2}{L^2}\sum_{k,\varepsilon_n}\frac{\Delta^*(i\omega_\lambda+2\xi_k)}{\{(i\varepsilon_n+i\omega_\lambda)^2-E_k^2\}\{(i\varepsilon_n)^2-E_k^2\}}\mathcal{D}_{++}(0,i\omega_\lambda)\sum_{k',\varepsilon_n'}\frac{\Delta(i\omega_\lambda+2\xi_{k'})}{\{(i\varepsilon_n'+i\omega_\lambda)^2-E_{k'}^2\}\{(i\varepsilon_n')^2-E_{k'}^2\}}, \quad (21)$$

where $\sigma_\pm = (\sigma_x \pm i\sigma_y)/2$ and $\sigma_x, \sigma_y, \sigma_z$ are 2×2 Pauli matrices. In the last expression, the terms proportional to ξ_k and $\xi_{k'}$ in the numerator vanish since they are odd functions of k and k', respectively. Figures 1(b)–1(d) can be calculated similarly, and their total becomes

$$\Phi_{11}(i\omega_\lambda) = -4e^2v_{\rm F}^2g_Q^2\Delta_0^2(i\omega_\lambda)^2\left[\frac{k_{\rm B}T}{L}\sum_{k,\varepsilon_n}\frac{1}{\{(i\varepsilon_n+i\omega_\lambda)^2-E_k^2\}\{(i\varepsilon_n)^2-E_k^2\}}\right]^2$$

$$\times\{\mathcal{D}_{++}(0,i\omega_\lambda) - e^{-2i\phi}\mathcal{D}_{+-}(0,i\omega_\lambda) - e^{2i\phi}\mathcal{D}_{-+}(0,i\omega_\lambda) + \mathcal{D}_{--}(0,i\omega_\lambda)\}. \quad (22)$$

Noting that $\mathcal{D}_{--} = \mathcal{D}_{++}$ and $\mathcal{D}_{-+} = e^{-4i\phi}\mathcal{D}_{+-}$ (see Appendix A), we see that the last set of parentheses in Eq. (22) is equal to twice the phason propagator $P(0, i\omega_\lambda)$.

In the lowest order of $i\omega_\lambda$ and $T \to 0$, the k summation and the Matsubara frequency summation in Eq. (22) can be carried out as

$$\frac{k_{\rm B}T}{L}\sum_{k,\varepsilon_n}\frac{1}{\{(i\varepsilon_n)^2-E_k^2\}^2} = -\frac{1}{L}\sum_k\int\frac{dz}{2\pi i}f(z)\frac{1}{(z^2-E_k^2)^2}$$

$$= \frac{1}{L}\sum_k\frac{1}{4E_k^3} = \frac{1}{4\pi\hbar|v_{\rm F}|\Delta_0^2}. \quad (23)$$

Therefore, the conductivity is given by

$$\sigma(\omega) = \frac{i\omega}{2}\left(\frac{e}{\pi}\right)^2\frac{g_Q^2}{\Delta_0^2}P(0,\hbar\omega+i\delta). \quad (24)$$

Equation (24) together with Eq. (15) leads to $\sigma(\omega) = n_e e^2/i\omega m^*$, with $m^* = [(1+X)/X]m$ and $n_e = 2k_F/\pi$, which is the result by LRA for the sliding phason mode contribution to the conductivity in clean systems, representing the perfect conductivity of the Fröhlich superconductivity. In the presence of impurities, which is always the case, phasons are pinned, resulting in vanishing static conductivity at absolute zero (see Appendix F).

So far we have reviewed in detail the derivation of phason contributions to L_{11} in order to make transparent and solid
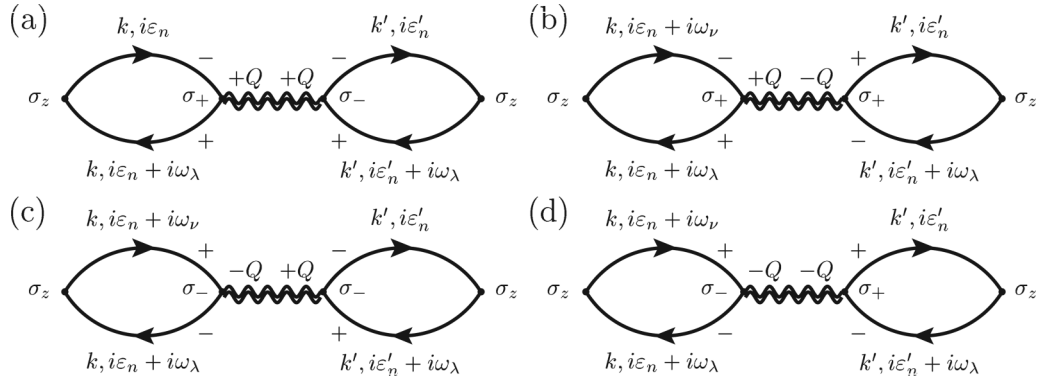
FIG. 1. Feynman diagrams for conductivity due to phasons. The solid lines and the wavy lines represent electron and phonon Green's functions, respectively, The $+$ and $-$ signs attached to the solid lines represent the subscripts of electron Green's functions $\mathcal{G}_{mn}$ with $m, n = \pm$, and the $+Q$ and $-Q$ attached to the wavy lines represent the subscripts of phonon Green's functions $\mathcal{D}_{mn}$.

the new contributions of phason drag to L_{12} on equal footing, which are explained in the following.

IV. THERMOELECTRIC CONDUCTIVITY DUE TO PHASON DRAG

In this section, we study the phason drag contribution to the thermoelectric conductivity L_{12}^{ph}, which is given by

$$L_{12}^{\mathrm{ph}} = \lim_{\omega \to 0} \frac{1}{i\omega} \left[\Phi_{12}^{\mathrm{ph}}(i\omega_\lambda \to \hbar\omega + i\delta) - \Phi_{12}^{\mathrm{ph}}(0) \right], \quad (25)$$

with

$$\Phi_{12}^{\mathrm{ph}}(i\omega_\lambda) = \frac{1}{L} \int_0^\beta d\tau \langle T_\tau [J_{\mathrm{h}}^{\mathrm{ph}}(\tau) J_e(0)] \rangle e^{i\omega_\lambda \tau}, \quad (26)$$

where $J_{\mathrm{h}}^{\mathrm{ph}}$ is the heat current carried by phonons [6],

$$J_{\mathrm{h}}^{\mathrm{ph}} = \sum_q \hbar\omega_q c_q b_q^\dagger b_q, \quad (27)$$

with $c_q = d\omega_q/dq$ being the phonon group velocity.

A. Phason drag process

As in the case of FeSb$_2$ [7], processes associated with phason drag are shown diagrammatically in Appendix C. Here, it should be noted that phonon propagators appearing in the phason drag processes are "directed" as fermions [6,7,21–25]; that is, instead of $\mathcal{D}_{mn}(q, \tau)$, we have to use $O_{mn}(q, \tau)$ defined as

$$O_{mn}(q, \tau) = -\langle T_\tau \{ b_{mQ+q}(\tau) [b_{nQ+q}^\dagger(0) + b_{-nQ-q}(0)] \} \rangle. \quad (28)$$

Details of the calculations are shown in Appendixes B and C. Finally, we obtain

$$\Phi_{12}^{\mathrm{ph}}(i\omega_\lambda) = e\hbar v_{\mathrm{F}} \omega_Q c_Q g_Q^2 \frac{(k_{\mathrm{B}}T)^2}{L^2} \sum_{k,q,n,\nu} \frac{i\omega_\nu + \hbar\omega_Q}{2\hbar\omega_Q} \frac{i\omega_\nu + i\omega_\lambda + \hbar\omega_Q}{2\hbar\omega_Q} \frac{1}{(i\varepsilon_n)^2 - E_k^2} \frac{1}{(i\varepsilon_n + i\omega_\lambda)^2 - E_k^2}$$

$$\times \{ P(q, i\omega_\nu) A(q, i\omega_\nu + i\omega_\lambda) + A(q, i\omega_\nu) P(q, i\omega_\nu + i\omega_\lambda) \}$$

$$\times \left[\{ f(q, i\omega_\nu + i\omega_\lambda) - f(-q, -i\omega_\nu) \} \{ i\varepsilon_n(i\varepsilon_n + i\omega_\lambda) + \xi_k^2 - \Delta_0^2 \} \right.$$

$$\left. - \{ g(q, i\omega_\nu + i\omega_\lambda) - g(-q, -i\omega_\nu) \} \xi_k(2i\varepsilon_n + i\omega_\lambda) \right] + O((i\omega_\lambda)^2), \quad (29)$$

with

$$f(q, i\omega_\nu) = \frac{i\varepsilon_n + i\omega_\nu}{(i\varepsilon_n + i\omega_\nu)^2 - E_{k+q}^2},$$

$$g(q, i\omega_\nu) = \frac{\xi_{k+q}}{(i\varepsilon_n + i\omega_\nu)^2 - E_{k+q}^2}. \quad (30)$$

From Eq. (10) we see that $\mathcal{D}_{mn}(-q, -i\omega_\nu) = \mathcal{D}_{mn}(q, i\omega_\nu)$, i.e., $P(-q, -i\omega_\nu) = P(q, i\omega_\nu)$ and $A(-q, -i\omega_\nu) = A(q, i\omega_\nu)$. Thus, changing variables, $q \to -q$ and $i\omega_\nu \to -i\omega_\nu - i\omega_\lambda$ in $f(-q, -i\omega_\nu)$ and $g(-q, -i\omega_\nu)$ in Eq. (29), we obtain

$$\Phi_{12}^{\mathrm{ph}}(i\omega_\lambda) = e\hbar v_{\mathrm{F}} \omega_Q c_Q g_Q^2 \frac{(k_{\mathrm{B}}T)^2}{L^2} \sum_{k,q,n,\nu} \frac{2i\omega_\nu + i\omega_\lambda}{2\hbar\omega_Q} \frac{1}{(i\varepsilon_n)^2 - E_k^2} \frac{1}{(i\varepsilon_n + i\omega_\lambda)^2 - E_k^2}$$

$$\times \{ P(q, i\omega_\nu) A(q, i\omega_\nu + i\omega_\lambda) + A(q, i\omega_\nu) P(q, i\omega_\nu + i\omega_\lambda) \}$$

$$\times \left[f(q, i\omega_\nu + i\omega_\lambda) \{ i\varepsilon_n(i\varepsilon_n + i\omega_\lambda) + \xi_k^2 - \Delta_0^2 \} - g(q, i\omega_\nu + i\omega_\lambda) \xi_k(2i\varepsilon_n + i\omega_\lambda) \right] + O((i\omega_\lambda)^2). \quad (31)$$

B. Analytic continuation and low-temperature properties of Φ_{12}^{ph}

For the static thermoelectric conductivity, we need to calculate the linear order of $i\omega_\lambda$ of Eq. (31), whose leading contributions are due to the region of $-\omega_\lambda < \omega_\nu < 0$. [The other regions give contributions proportional to $P(q, x + i\delta)A(q, x + i\delta)$ or $P(q, x - i\delta)A(q, x - i\delta)$, which will be in the higher order with respect to damping of the phason and amplitude mode.] After analytic continuation of $i\omega_\lambda \to \hbar\omega + i\delta$, we obtain

$$\Phi_{12}^{ph}(\hbar\omega + i\delta) = e\hbar v_F \omega c_Q g_Q^2 \frac{1}{L} \sum_q \int_{-\infty}^{\infty} \frac{dx}{2\pi i} n'(x)x\{P(q, x - i\delta)A(q, x + i\delta) + A(q, x - i\delta)P(q, x + i\delta)\}C(x, q) + O(\omega^2),$$

(32)

where

$$C(x, q) = \frac{k_B T}{L} \sum_{k,n} \frac{1}{\left[(i\varepsilon_n)^2 - E_k^2\right]^2} \frac{1}{(i\varepsilon_n + x)^2 - E_{k+q}^2} \left\{(i\varepsilon_n + x)\left\{(i\varepsilon_n)^2 + \xi_k^2 - \Delta_0^2\right\} - 2i\varepsilon_n \xi_k \xi_{k+q}\right\}.$$

(33)

By noting that $C(x, q)$ is due to fermionic contributions with energy and momenta higher than those of phonons, we expand $C(x, q)$ in terms of both x and q. In the lowest order with respect to q,

$$C(x, q) \sim C(x, 0) = \frac{k_B T}{L} \sum_{k,n} \frac{1}{\left[(i\varepsilon_n)^2 - E_k^2\right]^2} \frac{1}{(i\varepsilon_n + x)^2 - E_k^2} \left\{(i\varepsilon_n + x)\left\{(i\varepsilon_n)^2 + \xi_k^2 - \Delta_0^2\right\} - 2i\varepsilon_n \xi_k^2\right\}.$$

(34)

Since $n'(x)x$ is an odd function of x, the lowest order contributing to Eq. (32) is $C(x, 0) \sim xD(T)$, with

$$D(T) = -\frac{k_B T}{L} \sum_{k,n} \frac{(i\varepsilon_n)^2 - \xi_k^2 + \Delta_0^2}{\left[(i\varepsilon_n)^2 - E_k^2\right]^3}.$$

(35)

Equation (35) is derived also rather straightforwardly by putting $q = 0$ and $i\omega_\lambda = 0$ in the electron Green's functions in Fig. 4 (see Appendix D). Finally, the static thermoelectric conductivity at low temperature $L_{12}^{ph}(T)$ is given as follows:

$$L_{12}^{ph}(T) = -e\hbar v_F c_Q g_Q^2 \frac{D(T)}{L} \sum_q \int_{-\infty}^{\infty} \frac{dx}{2\pi} n'(x)x^2\{P(q, x - i\delta)A(q, x + i\delta) + A(q, x - i\delta)P(q, x + i\delta)\}.$$

(36)

At $T = 0$, $D(0) = k_F/8\pi E_{k_F}^3$, which is shown in Appendix E. We see that L_{12} is governed by both phase and amplitude modes, while L_{11} is governed by only the phase mode. Although impurity scattering affects both modes, phasons are more sensitive, which has been studied before in the context of impurity pinning, which will be briefly summarized in the following.

C. General features of phason propagators

In order to explore the implication of Eq. (36), we analyze the propagators of collective modes of phason and amplitude, $P(q, \hbar\omega + i\delta)$ and $A(q, \hbar\omega + i\delta)$, given by Eq. (15) with TTF-TCNQ in mind in the impurity-pinned state, i.e., in the charge density glass (CDG) state instead of the CDW state. We note that phonon propagators in glasses are proposed to be of the following type, e.g., in Ref. [26]:

$$P(q, \hbar\omega + i\delta) = \frac{2\hbar\omega_Q/(1 + X)}{(\hbar\omega + i\delta)^2 - \hbar^2\omega_{ph}^2(q) + i\hbar\omega\Gamma_{ph}},$$

$$A(q, \hbar\omega + i\delta) = \frac{2\hbar\omega_Q/(1 + X/3)}{(\hbar\omega + i\delta)^2 - \hbar^2\omega_{am}^2(q) + i\hbar\omega\Gamma_{am}},$$

(37)

where $\omega_{ph}(q) = v|q|$ and $\omega_{am}(q)$ are the dispersions of the phason and the amplitude mode, respectively. Γ_{ph} and Γ_{am} reflect the effects of randomness. This expectation is justified for the amplitude mode, which is optical and has a finite

gap at $q = 0$. However, this expectation is totally invalid for the phason, which is acoustic. In the following we will see that $P(q, \hbar\omega + i\delta)$ is greatly modified because of the impurity pinning.

We first note that these modes derived by the mean-field theory should be valid in the three-dimensionally ordered Peierls phase. The critical temperature to the ordered Peierls phase is $T_P \sim 54$ K, which is believed to be much lower than the mean-field transition temperature $T_{P0} \sim 500$ K [27] because of strong fluctuations intrinsic to one-dimensionality. The wave number q is measured relative to $2k_F$ since these are phonon modes in the Peierls phase with the long-range order parameter of the coherent lattice distortion with period $2k_F = Q$. As clarified by LRA, phasons carry charge current, while amplitude modes are neutral. This implies that phasons are considered to be charged phonons. Hence, the present phasons have particular features compared with ordinary phonons: very low energy and sensitivity to spatial randomness because of the charged object.

The subtle problem of the coupling of phasons to spatial randomness leading to impurity pinning had been studied before based on the effective Hamiltonian, the phase Hamiltonian [18,19], which indicates that $P(q, \hbar\omega + i\delta)$ (37) at absolute zero is modified as follows:

$$P(q, \hbar\omega + i\delta) = \frac{2\hbar\omega_Q/(1 + X)}{(\hbar\omega + i\delta)^2 - \hbar^2 v^2 q^2 - g_0 + i\hbar\omega g_1}, \quad (38)$$

where g_0 ($\sim \gamma^2$) and g_1 ($\sim \gamma$) are parameters associated with the impurity pinning potential γ ($\gamma > 0$; for details, see Appendix F).

From Eq. (38) with finite g_0, it is seen that $\sigma(\omega) \sim i\omega$ as $\omega \to 0$, which is the characteristic of dielectrics (insulators) with the dielectric constant $\varepsilon(\omega) = 1 + 4\pi i \sigma(\omega)/\omega \sim 1/(g_0 - i\hbar\omega g_1)$. This reflects the fact that Peierls lattice distortions are no longer uniform in the pinned CDW state and that the spatial charge density is disordered, i.e., glassy. In such a glassy state, the CDG state [28], the possible charge transport is either uniform oscillations of phasons within each domain or local variation of phase associated with domain walls described as solitons, both of which need finite excitation energy. These are features of impurity pinning at $T = 0$ for finite frequency $\omega \neq 0$.

At finite temperature, $T \neq 0$, these low-energy excitations are thermally excited, resulting in small, but finite, conductivity, which implies $g_0 = 0$ with finite g_1 in Eq. (38). There will be an interesting crossover from the zero-temperature value of g_0 to vanishing g_0 at finite temperature, and this is associated with the dielectric anomalies which have characteristic dependences on both the frequency and temperature of the dielectric constant in some family of molecular solids [29]. But this issue is beyond the scope of the present paper. In the following, we assume $g_0 = 0$ for $T > 0$. In this case, the static conductivity σ_0 is given by

$$\sigma_0 = \left(\frac{e}{\pi}\right)^2 \frac{g_Q^2}{(1+X)\Delta_0^2} \frac{\omega_Q}{g_1}. \tag{39}$$

In the present context of TTF-TCNQ experiments indicate more or less the activation type of the temperature dependence of the conductivity [16], implying $g_1(T) \sim \gamma \exp(E_0/k_B T)$, which we will assume in the following.

D. The temperature dependences of $L_{12}^{ph}(T)$

In order to see the implication of (36), we first note the dispersion of the amplitude mode $\omega_{am}(q)$ is relatively weak compared to that of phasons: we assume $\omega_{am}(q)$ is a q-independent constant, ω_a. Then, q integration in Eq. (36) is possible analytically, leading to

$$
\begin{aligned}
F(x, T) &= \frac{1}{L} \sum_q \left\{ P(q, x - i\delta) A(q, x + i\delta) + A(q, x - i\delta) P(q, x + i\delta) \right\} \\
&= 2\mathrm{Re} \int_{-\infty}^{\infty} \frac{dq}{2\pi} \left(\frac{2\hbar\omega_Q/(1+X)}{x^2 - \hbar^2 v^2 q^2 - ig_1 x} \right) \left(\frac{2\hbar\omega_Q/(1+X/3)}{x^2 - \hbar^2 \omega_{am}^2 + ix\Gamma_{am}} \right) \\
&= -\mathrm{Re} \left[\frac{4i\hbar\omega_Q^2/v(1+X)(1+X/3)}{(x^2 - \hbar^2 \omega_a^2 + ix\Gamma_{am})(x^2 - ig_1 x)^{1/2}} \right],
\end{aligned}
\tag{40}
$$

where the argument of $(x^2 - ig_1 x)^{1/2}$ is chosen to be $\mathrm{Im}(x^2 - ig_1 x)^{1/2} > 0$. Therefore, $L_{12}^{ph}(T)$ in Eq. (36) becomes

$$L_{12}^{ph}(T) = -e\hbar^2 v_F c_Q g_Q^2 D(T) \int_{-\infty}^{\infty} \frac{dx}{2\pi} n'(x) x^2 F(x, T). \tag{41}$$

It should be noted that the factor $|n'(x)|$ is large only for $|x| \lesssim k_B T$ at low temperatures.

As discussed in the previous section, when the system is conductive, we expect $g_1 \sim \gamma \exp(E_0/k_B T)$. In the low temperatures where $g_1 \gg k_B T$ holds, $F(x, T)$ is approximated as

$$F(x, T) = \frac{4\omega_Q^2}{\sqrt{2}\hbar v \omega_a^2 (1+X)(1+X/3)} \frac{1}{\sqrt{g_1(T)|x|}}, \tag{42}$$

and then

$$
\begin{aligned}
L_{12}^{ph}(T) &= \frac{e\hbar v_F c_Q g_Q^2 \omega_Q^2}{\sqrt{2}\pi v \omega_a^2 (1+X)(1+X/3)} \frac{(k_B T)^{3/2}}{\sqrt{g_1(T)}} D(T) \int_0^{\infty} dz \frac{z^{3/2}}{\sinh^2 z} \\
&= 2.936 \frac{e\hbar v_F c_Q g_Q^2 \omega_Q^2}{\sqrt{2}\pi v \omega_a^2 (1+X)(1+X/3)} \frac{(k_B T)^{3/2}}{\sqrt{g_1(T)}} D(T),
\end{aligned}
\tag{43}
$$

which leads to

$$S = \frac{L_{12}^{ph}}{T\sigma} \propto v_F c_Q T^{1/2} e^{E_0/2k_B T}. \tag{44}$$

Here, $D(T)$ has been approximated as a constant, $D(0)$.

It should be noted that $|S|$ is exponentially diverging toward absolute zero in the present one-dimensional (1D) Peierls model, where the energy dispersion of the electronic band is strictly 1D. The sign of S is determined by $c_Q = d\omega_q/dq|_{q=Q}$ ($Q = 2k_F$) since $v_F > 0$ is independent of the filling of the band in the present 1D electron model: $S > 0$ for $0 < Q < G/2$ ("electrons") and $S < 0$ for $G/2 < Q < G$ ("holes"), with G being the reciprocal lattice vectors. In the case of the charge transfer salts that interest us, TTF-TCNQ, however,

the system is semimetallic with the same number of electrons and holes in the TCNQ band and the TTF band, and then $v_F > 0$ for electrons, and $v_F < 0$ for holes, as in doped semiconductors.

The present results may point to an interesting possibility of thermoelectricity in disordered (glassy) systems with strong electron-phonon coupling between low-temperature insulating and weakly conducting intermediate-temperature regions which may include some cases of variable range hopping.

V. SUMMARY

In the present paper, the effects of phason drag on the Seebeck coefficient were theoretically studied for the one-dimensional incommensurate Peierls phase with TTF-TCNQ in mind based on the Kubo-Luttinger formalism with the help of thermal Green's function. The phason is the collective mode of electron-lattice coupled CDW systems and represents the sliding motions of electronic charge density and lattice distortion as clarified by LRA. Hence, phasons can be considered the ultimate form of phonon drag, which has long been known to play important roles in semiconductors and was found to also do so in $FeSb_2$ recently.

In order to treat phason dynamics theoretically, it is crucial to note the existence of two energy scales, i.e., the high-energy region representing electronic degrees of freedom to support the Peierls phase and the low-energy region describing the collective modes (amplitude and phase modes) in the Peierls ordered state. As demonstrated by LRA, phasons are charged, while amplitude modes are neutral. Phasons, which represent sliding motions of coupled electronic charge density and lattice distortions, have acoustic wave vector dependence and lead to perfect electric conduction (Fröhlich superconductivity) in clean systems. However, phasons are sensitive to spatial inhomogeneity, in contrast to the phase of superconductivity, and are easily pinned by impurities, resulting in an insulating state at absolute zero with inhomogeneous spatial charge density, i.e., a charge density glass state. In order to describe this dramatic process of pinning from perfect conduction to the insulating CDG state the phase Hamiltonian, which is an effective Hamiltonian focusing on phasons, is known to be powerful to see the frequency dependences of conductivity at $T = 0$. In the present studies on the Seebeck coefficient we need to extend this study to finite temperatures.

We first demonstrated the perfect correspondences between former diagrammatical calculations of conductivity L_{11} and thermoelectric conductivity L_{12} and those based on the phase Hamiltonian in the absence of pining. Then the effects of pinning on phasons governing L_{11} at finite temperatures were analyzed based on previous analysis at absolute zero (but finite frequencies). This partly corresponds to general studies on phonon propagators in disordered systems, i.e., phonons in glassy states. However, there is an important difference between phonons in a glassy state and the present CDG state: phonons are neutral in the former, while they are charged here. In the CDG state the dependences on frequency and temperature of phasons are more subtle than in neutral phonons. With such detailed studies on phason propagators in the CDG state, its drag effects on L_{12} and then $S = L_{12}/T L_{11}$ have been identified. It turns out that $|S|$ can be very large: When conductivity obeys the Arrhenius type of temperature dependence, $L_{11} \propto e^{-E_0/k_B T}$, then $L_{12}^{ph} \propto v_F c_Q T^{3/2} e^{-E_0/2k_B T}$, and $S \propto v_F c_Q T^{1/2} e^{E_0/2k_B T}$ as $T \to 0$. The sign of S is always opposite that of electronic contributions, which appear to be consistent with experiments [30], although the description of crossover regions between high temperature with electronic contributions and the present low temperatures deep in the Peierls ordered state is beyond the scope of the present paper.

The main result of this paper is the identification of the phason drag contribution to the thermoelectric conductivity L_{12}, Eq. (36), in terms of phason and amplitude propagators, $P(q, x)$ and $A(q, x)$, to be combined with the conductivity L_{11}, Eq. (24), for the Peierls phase treated within the mean-field theory. Even if the Peierls phase is treated in more detail beyond the mean-field theory, the main framework of the present scheme will be valid for the contribution of phase and amplitude modes as long as the Peierls phase is long range ordered and stable with possible modifications of the prefactors of Eqs. (24) and (36).

APPENDIX A: DYSON EQUATIONS FOR PHONON PROPAGATORS

The Dyson equations for $\mathcal{D}_{mn}$ by LRA are shown in Fig. 2:

$$\mathcal{D}_{++}(q, i\omega_\nu) = \mathcal{D}_{++}^{(0)}(q, i\omega_\nu) + \mathcal{D}_{++}(q, i\omega_\nu)\Pi_{++}(q, i\omega_\nu)\mathcal{D}_{++}^{(0)}(q, i\omega_\nu) + \mathcal{D}_{+-}(q, i\omega_\nu)\Pi_{-+}(q, i\omega_\nu)\mathcal{D}_{++}^{(0)}(q, i\omega_\nu),$$

$$\mathcal{D}_{+-}(q, i\omega_\nu) = \mathcal{D}_{++}(q, i\omega_\nu)\Pi_{+-}(q, i\omega_\nu)\mathcal{D}_{--}^{(0)}(q, i\omega_\nu) + \mathcal{D}_{+-}(q, i\omega_\nu)\Pi_{--}(q, i\omega_\nu)\mathcal{D}_{--}^{(0)}(q, i\omega_\nu),$$

$$\mathcal{D}_{-+}(q, i\omega_\nu) = \mathcal{D}_{--}(q, i\omega_\nu)\Pi_{-+}(q, i\omega_\nu)\mathcal{D}_{++}^{(0)}(q, i\omega_\nu) + \mathcal{D}_{-+}(q, i\omega_\nu)\Pi_{++}(q, i\omega_\nu)\mathcal{D}_{++}^{(0)}(q, i\omega_\nu),$$

$$\mathcal{D}_{--}(q, i\omega_\nu) = \mathcal{D}_{--}^{(0)}(q, i\omega_\nu) + \mathcal{D}_{--}(q, i\omega_\nu)\Pi_{--}(q, i\omega_\nu)\mathcal{D}_{--}^{(0)}(q, i\omega_\nu) + \mathcal{D}_{-+}(q, i\omega_\nu)\Pi_{+-}(q, i\omega_\nu)\mathcal{D}_{--}^{(0)}(q, i\omega_\nu), \quad \text{(A1)}$$

where Π_{mn} are defined in Eq. (11). It should be noted that the relations $\Pi_{++} = \Pi_{--}$ and $\Pi_{-+} = e^{-4i\phi}\Pi_{+-}$ hold from their definitions. (Note that in the presence of $\overline{\varepsilon}_k$ the relation $\Pi_{++} = \Pi_{--}$ does not hold.) Furthermore, when we use the
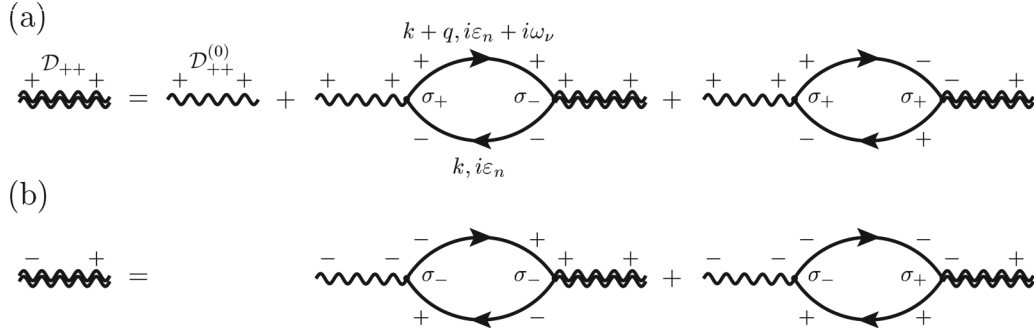
FIG. 2. Feynman diagrams of Dyson equations for the phonon propagator $\mathcal{D}_{mn}$. The wavy line (the wavy double line) represents $\mathcal{D}_{mn}^{(0)}$ ($\mathcal{D}_{mn}$). The $+$ and $-$ signs attached to the wavy lines and the solid lines represent the subscripts of the corresponding propagator. The Dyson equations for $\mathcal{D}_{--}$ and $\mathcal{D}_{-+}$ are written in the same way.

approximation [Eq. (13)]

$$\mathcal{D}_{mn}^{(0)}(q, i\omega_\nu) \sim \delta_{mn}\mathcal{D}^{(0)}(i\omega_\nu) = \delta_{mn}\frac{2\hbar\omega_Q}{(i\omega_\nu)^2 - \hbar^2\omega_Q^2}, \tag{A2}$$

Eq. (A1) becomes

$$\mathcal{D}_{++}(q, i\omega_\nu) = \left\{1 + \mathcal{D}_{++}(q, i\omega_\nu)\Pi_{++}(q, i\omega_\nu) + \mathcal{D}_{+-}(q, i\omega_\nu)e^{-4i\phi}\Pi_{+-}(q, i\omega_\nu)\right\}\mathcal{D}^{(0)}(i\omega_\nu),$$

$$\mathcal{D}_{+-}(q, i\omega_\nu) = \left\{\mathcal{D}_{++}(q, i\omega_\nu)\Pi_{+-}(q, i\omega_\nu) + \mathcal{D}_{+-}(q, i\omega_\nu)\Pi_{++}(q, i\omega_\nu)\right\}\mathcal{D}^{(0)}(i\omega_\nu),$$

$$\mathcal{D}_{-+}(q, i\omega_\nu) = \left\{\mathcal{D}_{--}(q, i\omega_\nu)e^{-4i\phi}\Pi_{+-}(q, i\omega_\nu) + \mathcal{D}_{-+}(q, i\omega_\nu)\Pi_{++}(q, i\omega_\nu)\right\}\mathcal{D}^{(0)}(i\omega_\nu),$$

$$\mathcal{D}_{--}(q, i\omega_\nu) = \left\{1 + \mathcal{D}_{--}(q, i\omega_\nu)\Pi_{++}(q, i\omega_\nu) + \mathcal{D}_{-+}(q, i\omega_\nu)\Pi_{+-}(q, i\omega_\nu)\right\}\mathcal{D}^{(0)}(i\omega_\nu). \tag{A3}$$

From these Dyson equations, we can see that

$$\mathcal{D}_{++}(q, i\omega_\nu) \pm e^{-2i\phi}\mathcal{D}_{+-}(q, i\omega_\nu) = \left[1 + \left\{\mathcal{D}_{++}(q, i\omega_\nu) \pm e^{-2i\phi}\mathcal{D}_{+-}(q, i\omega_\nu)\right\}\left\{\Pi_{++}(q, i\omega_\nu) \pm e^{-2i\phi}\Pi_{+-}(q, i\omega_\nu)\right\}\right]\mathcal{D}^{(0)}(i\omega_\nu), \tag{A4}$$

which leads to Eq. (10). In a similar way, we obtain $\mathcal{D}_{--} = \mathcal{D}_{++}$ and $\mathcal{D}_{-+} = e^{-4i\phi}\mathcal{D}_{+-}$.

The phason propagator $P(q, i\omega_\nu)$ in Eq. (14) is evaluated in the small-q and small-$(i\omega_\nu)$ region as follows. Substituting the definition of $\mathcal{D}^{(0)}(q, i\omega_\nu)$, $P(q, i\omega_\nu)$ is rewritten as

$$P(q, i\omega_\nu) = \frac{2\hbar\omega_Q}{(i\omega_\nu)^2 - (\hbar\omega_Q)^2 - 2\hbar\omega_Q[\Pi_{++}(q, i\omega_\nu) - e^{-2i\phi}\Pi_{+-}(q, i\omega_\nu)]}. \tag{A5}$$

Using the definition in Eq. (11) and the Green's function in Eq. (9), we obtain

$$\Pi_{++}(q, i\omega_\nu) - e^{-2i\phi}\Pi_{+-}(q, i\omega_\nu) = 2g_Q^2\frac{k_B T}{L}\sum_{k,n}\frac{(i\varepsilon_n + i\omega_\nu + \xi_{k+q})(i\varepsilon_n - \xi_k) - \Delta_0^2}{\left[(i\varepsilon_n + i\omega_\nu)^2 - E_{k+q}^2\right]\left[(i\varepsilon_n)^2 - E_k^2\right]}. \tag{A6}$$

When $q = 0$ and $i\omega_\nu = 0$, the right-hand side of Eq. (A6) becomes

$$2g_Q^2\frac{k_B T}{L}\sum_{k,n}\frac{1}{(i\varepsilon_n)^2 - E_k^2} = -2g_Q^2\frac{1}{L}\sum_k\oint\frac{dz}{2\pi i}\frac{f(z)}{z^2 - E_k^2}$$

$$= 2g_Q^2\frac{1}{L}\sum_k\frac{f(E_k) - f(-E_k)}{2E_k}$$

$$= -\frac{\hbar\omega_Q}{2}, \tag{A7}$$

where the self-consistency equation in Eq. (4) has been used. The phason velocity is obtained by calculating the higher-order terms with respect to q and $i\omega_\nu$. It is straightforward to obtain

$$\Pi_{++}(q, i\omega_\nu) - e^{-2i\phi}\Pi_{+-}(q, i\omega_\nu) = -\frac{\hbar\omega_Q}{2} + \frac{X(\hbar v_F q)^2}{2\hbar\omega_Q} - \frac{X(i\omega_\nu)^2}{2\hbar\omega_Q} + (\text{higher-order terms}), \tag{A8}$$
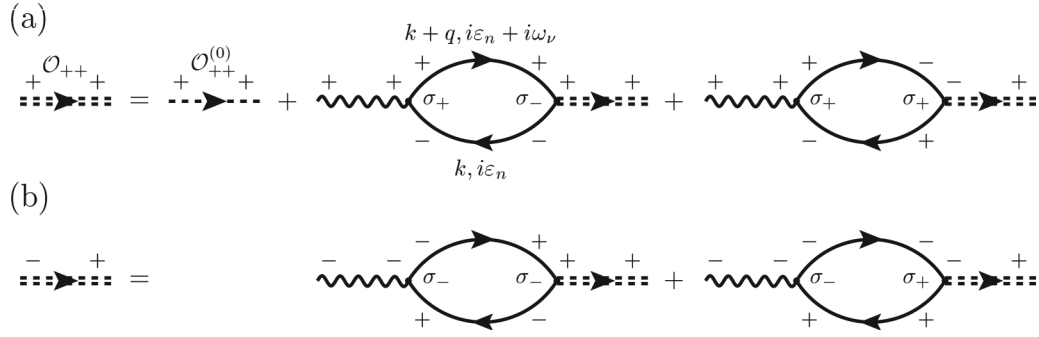
FIG. 3. Feynman diagrams of Dyson equations for the "directed" phonon propagator O_{mn}. The dashed line (the double-dashed line) with an arrow represents $O_{mn}^{(0)}$ (O_{mn}). The $+$ and $-$ signs attached to the dashed lines and the solid lines represent the subscripts of the corresponding propagator. The Dyson equations for O_{--} and O_{-+} are written in the same way.

with

$$X = \frac{\omega_Q g_Q^2}{2\pi |v_F| \Delta_0^2}. \tag{A9}$$

Substituting (A8) into (A5), the phason propagator becomes

$$
\begin{aligned}
P(q, i\omega_v) &= \frac{2\hbar\omega_Q}{(i\omega_v)^2 - X(\hbar v_F q)^2 + X(i\omega_v)^2} \\
&= \frac{2\hbar\omega_Q/(1+X)}{(i\omega_v)^2 - \frac{X}{1+X}(\hbar v_F q)^2} \\
&= \frac{2\hbar\omega_Q/(1+X)}{(i\omega_v)^2 - (\hbar v q)^2},
\end{aligned} \tag{A10}
$$

where v represents the phason velocity, defined as $v = [X/(1+X)]^{1/2}|v_F|$. In a similar way, we obtain

$$\Pi_{++}(q, i\omega_v) + e^{-2i\phi}\Pi_{+-}(q, i\omega_v) = -\frac{\hbar\omega_Q}{2} + \frac{2X\Delta_0^2}{\hbar\omega_Q} + \frac{X(\hbar v_F q)^2}{6\hbar\omega_Q} - \frac{X(i\omega_v)^2}{6\hbar\omega_Q} + \text{(higher-order terms)}. \tag{A11}$$

Therefore, the amplitude propagator becomes

$$
\begin{aligned}
A(q, i\omega_v) &= \frac{2\hbar\omega_Q}{(i\omega_v)^2 - 4X\Delta_0^2 - \frac{X}{3}(\hbar v_F q)^2 + \frac{X}{3}(i\omega_v)^2} \\
&= \frac{2\hbar\omega_Q/(1+X/3)}{(i\omega_v)^2 - \hbar^2\omega_{am}^2(q)},
\end{aligned} \tag{A12}
$$

with

$$\omega_{am}(q) = \sqrt{\frac{4X}{1+\frac{X}{3}}\Delta_0^2 + \frac{X}{3+X}(\hbar v_F q)^2}. \tag{A13}$$

APPENDIX B: DYSON EQUATIONS FOR "DIRECTED" PHONON PROPAGATORS

The Dyson equations for O_{mn} are shown in Fig. 3:

$$O_{++}(q, i\omega_v) = O_{++}^{(0)}(q, i\omega_v) + O_{++}(q, i\omega_v)\Pi_{++}(q, i\omega_v)\mathcal{D}_{++}^{(0)}(q, i\omega_v) + O_{+-}(q, i\omega_v)\Pi_{-+}(q, i\omega_v)\mathcal{D}_{++}^{(0)}(q, i\omega_v),$$

$$O_{+-}(q, i\omega_v) = O_{++}(q, i\omega_v)\Pi_{+-}(q, i\omega_v)\mathcal{D}_{--}^{(0)}(q, i\omega_v) + O_{+-}(q, i\omega_v)\Pi_{--}(q, i\omega_v)\mathcal{D}_{--}^{(0)}(q, i\omega_v),$$

$$O_{-+}(q, i\omega_v) = O_{--}(q, i\omega_v)\Pi_{-+}(q, i\omega_v)\mathcal{D}_{++}^{(0)}(q, i\omega_v) + O_{-+}(q, i\omega_v)\Pi_{++}(q, i\omega_v)\mathcal{D}_{++}^{(0)}(q, i\omega_v),$$

$$O_{--}(q, i\omega_v) = O_{--}^{(0)}(q, i\omega_v) + O_{--}(q, i\omega_v)\Pi_{--}(q, i\omega_v)\mathcal{D}_{--}^{(0)}(q, i\omega_v) + O_{-+}(q, i\omega_v)\Pi_{+-}(q, i\omega_v)\mathcal{D}_{--}^{(0)}(q, i\omega_v), \tag{B1}$$

where $O_{mn}^{(0)}(q, i\omega_\nu)$ are defined as

$$O_{mn}^{(0)}(q, i\omega_\nu) = \frac{\delta_{mn}}{i\omega_\nu - \hbar\omega_{mQ+q}}. \tag{B2}$$

Solving the Dyson equation for O_{mn}, we obtain the simple relations

$$O_{mn}(q, i\omega_\nu) = \frac{O^{(0)}(i\omega_\nu)}{\mathcal{D}^{(0)}(i\omega_\nu)}\mathcal{D}_{mn}(q, i\omega_\nu) = \frac{i\omega_\nu + \hbar\omega_Q}{2\hbar\omega_Q}\mathcal{D}_{mn}(q, i\omega_\nu), \tag{B3}$$

where it should be noted that we used an approximation,

$$O_{mn}^{(0)}(q, i\omega_\nu) \sim \delta_{mn}O^{(0)}(i\omega_\nu) = \delta_{mn}\frac{1}{i\omega_\nu - \hbar\omega_Q}, \tag{B4}$$

as for $\mathcal{D}_{mn}^{(0)}(q, i\omega_\nu)$. The same argument is applied to $\tilde{O}_{mn}(q, i\omega_\nu)$, which leads to $\tilde{O}_{mn}(q, i\omega_\nu) = O_{mn}(q, i\omega_\nu)$.

APPENDIX C: FEYNMAN DIAGRAMS FOR THE PHASON DRAG

The Feynman diagrams for the phason drag contributions $\Phi_{12}^{\text{ph}}(i\omega_\lambda)$ of Eq. (26) are shown in Fig. 4. Figures 4(a)–4(d) give, respectively,

$$-g_Q^2 \frac{(k_{\text{B}}T)^2}{L^2} \sum_{k,q,n,\nu} \hbar\omega_Q c_Q \tilde{O}_{++}(q, i\omega_\nu) O_{++}(q, i\omega_\nu + i\omega_\lambda) e v_{\text{F}} \text{Tr}[\mathcal{G}(k, i\varepsilon_n)\sigma_+ \mathcal{G}(k - q, i\varepsilon_n - i\omega_\nu)\sigma_- \mathcal{G}(k, i\varepsilon_n + i\omega_\lambda)\sigma_z]$$

$$= -g_Q^2 \frac{(k_{\text{B}}T)^2}{L^2} \sum_{k,q,n,\nu} \hbar\omega_Q c_Q \tilde{O}_{++}(q, i\omega_\nu) O_{++}(q, i\omega_\nu + i\omega_\lambda) e v_{\text{F}} \{\mathcal{G}_{++}(k, i\varepsilon_n)\mathcal{G}_{--}(k - q, i\varepsilon_n - i\omega_\nu)\mathcal{G}_{++}(k, i\varepsilon_n + i\omega_\lambda)$$

$$- \mathcal{G}_{-+}(k, i\varepsilon_n)\mathcal{G}_{--}(k - q, i\varepsilon_n - i\omega_\nu)\mathcal{G}_{+-}(k, i\varepsilon_n + i\omega_\lambda)\},$$

$$g_Q^2 \frac{(k_{\text{B}}T)^2}{L^2} \sum_{k,q,n,\nu} \hbar\omega_Q c_Q \tilde{O}_{+-}(q, i\omega_\nu) O_{-+}(q, i\omega_\nu + i\omega_\lambda) e v_{\text{F}} \text{Tr}[\mathcal{G}(k, i\varepsilon_n)\sigma_+ \mathcal{G}(k - q, i\varepsilon_n - i\omega_\nu)\sigma_- \mathcal{G}(k, i\varepsilon_n + i\omega_\lambda)\sigma_z]$$

$$= g_Q^2 \frac{(k_{\text{B}}T)^2}{L^2} \sum_{k,q,n,\nu} \hbar\omega_Q c_Q \tilde{O}_{+-}(q, i\omega_\nu) O_{-+}(q, i\omega_\nu + i\omega_\lambda) e v_{\text{F}} \{\mathcal{G}_{++}(k, i\varepsilon_n)\mathcal{G}_{--}(k - q, i\varepsilon_n - i\omega_\nu)\mathcal{G}_{++}(k, i\varepsilon_n + i\omega_\lambda)$$

$$- \mathcal{G}_{-+}(k, i\varepsilon_n)\mathcal{G}_{--}(k - q, i\varepsilon_n - i\omega_\nu)\mathcal{G}_{+-}(k, i\varepsilon_n + i\omega_\lambda)\},$$

$$-g_Q^2 \frac{(k_{\text{B}}T)^2}{L^2} \sum_{k,q,n,\nu} \hbar\omega_Q c_Q \tilde{O}_{++}(q, i\omega_\nu) O_{++}(q, i\omega_\nu + i\omega_\lambda) e v_{\text{F}} \text{Tr}[\mathcal{G}(k, i\varepsilon_n)\sigma_- \mathcal{G}(k + q, i\varepsilon_n + i\omega_\nu + i\omega_\lambda)\sigma_+ \mathcal{G}(k, i\varepsilon_n + i\omega_\lambda)\sigma_z]$$

$$= -g_Q^2 \frac{(k_{\text{B}}T)^2}{L^2} \sum_{k,q,n,\nu} \hbar\omega_Q c_Q \tilde{O}_{++}(q, i\omega_\nu) O_{++}(q, i\omega_\nu + i\omega_\lambda) e v_{\text{F}} \{\mathcal{G}_{+-}(k, i\varepsilon_n)\mathcal{G}_{++}(k + q, i\varepsilon_n + i\omega_\nu + i\omega_\lambda)\mathcal{G}_{-+}(k, i\varepsilon_n + i\omega_\lambda)$$

$$- \mathcal{G}_{--}(k, i\varepsilon_n)\mathcal{G}_{++}(k + q, i\varepsilon_n + i\omega_\nu + i\omega_\lambda)\mathcal{G}_{--}(k, i\varepsilon_n + i\omega_\lambda)\},$$

$$g_Q^2 \frac{(k_{\text{B}}T)^2}{L^2} \sum_{k,q,n,\nu} \hbar\omega_Q c_Q \tilde{O}_{+-}(q, i\omega_\nu) O_{-+}(q, i\omega_\nu + i\omega_\lambda) e v_{\text{F}} \text{Tr}[\mathcal{G}(k, i\varepsilon_n)\sigma_- \mathcal{G}(k + q, i\varepsilon_n + i\omega_\nu + i\omega_\lambda)\sigma_+ \mathcal{G}(k, i\varepsilon_n + i\omega_\lambda)\sigma_z]$$

$$= g_Q^2 \frac{(k_{\text{B}}T)^2}{L^2} \sum_{k,q,n,\nu} \hbar\omega_Q c_Q \tilde{O}_{+-}(q, i\omega_\nu) O_{-+}(q, i\omega_\nu + i\omega_\lambda) e v_{\text{F}} \{\mathcal{G}_{+-}(k, i\varepsilon_n)\mathcal{G}_{++}(k + q, i\varepsilon_n + i\omega_\nu + i\omega_\lambda)\mathcal{G}_{-+}(k, i\varepsilon_n + i\omega_\lambda)$$

$$- \mathcal{G}_{--}(k, i\varepsilon_n)\mathcal{G}_{++}(k + q, i\varepsilon_n + i\omega_\nu + i\omega_\lambda)\mathcal{G}_{--}(k, i\varepsilon_n + i\omega_\lambda)\}. \tag{C1}$$

$\omega_{\pm Q+q}$, $c_{\pm Q+q}$, and $g_{\pm Q+q}$ are approximated as ω_Q, $\pm c_Q$, and g_Q, respectively. Here, it should be noted that the phonon propagators are "directed" as fermions; that is, $O_{mn}(q, i\omega_\nu)$ and $\tilde{O}_{mn}(q, i\omega_\nu)$ are Fourier transforms of

$$O_{mn}(q, \tau) = -\langle T_\tau \{b_{mQ+q}(\tau)[b_{nQ+q}^\dagger(0) + b_{-nQ-q}(0)]\}\rangle,$$

$$\tilde{O}_{mn}(q, \tau) = -\langle T_\tau \{[b_{mQ+q}(\tau) + b_{-mQ-q}^\dagger(\tau)]b_{nQ+q}^\dagger(0)\}\rangle, \tag{C2}$$

respectively, with $m, n = \pm$.

For Figs. 4(e)–4(p), the $+$ and $-$ signs for $\mathcal{G}_{mn}$, O_{mn}, and $\tilde{O}_{mn}$ are different from those in diagrams Figs. 4(a)–4(d), while the momenta and Matsubara frequencies are the same. Noting that the electronic part is common in the Figs. 4(e) and 4(f), for
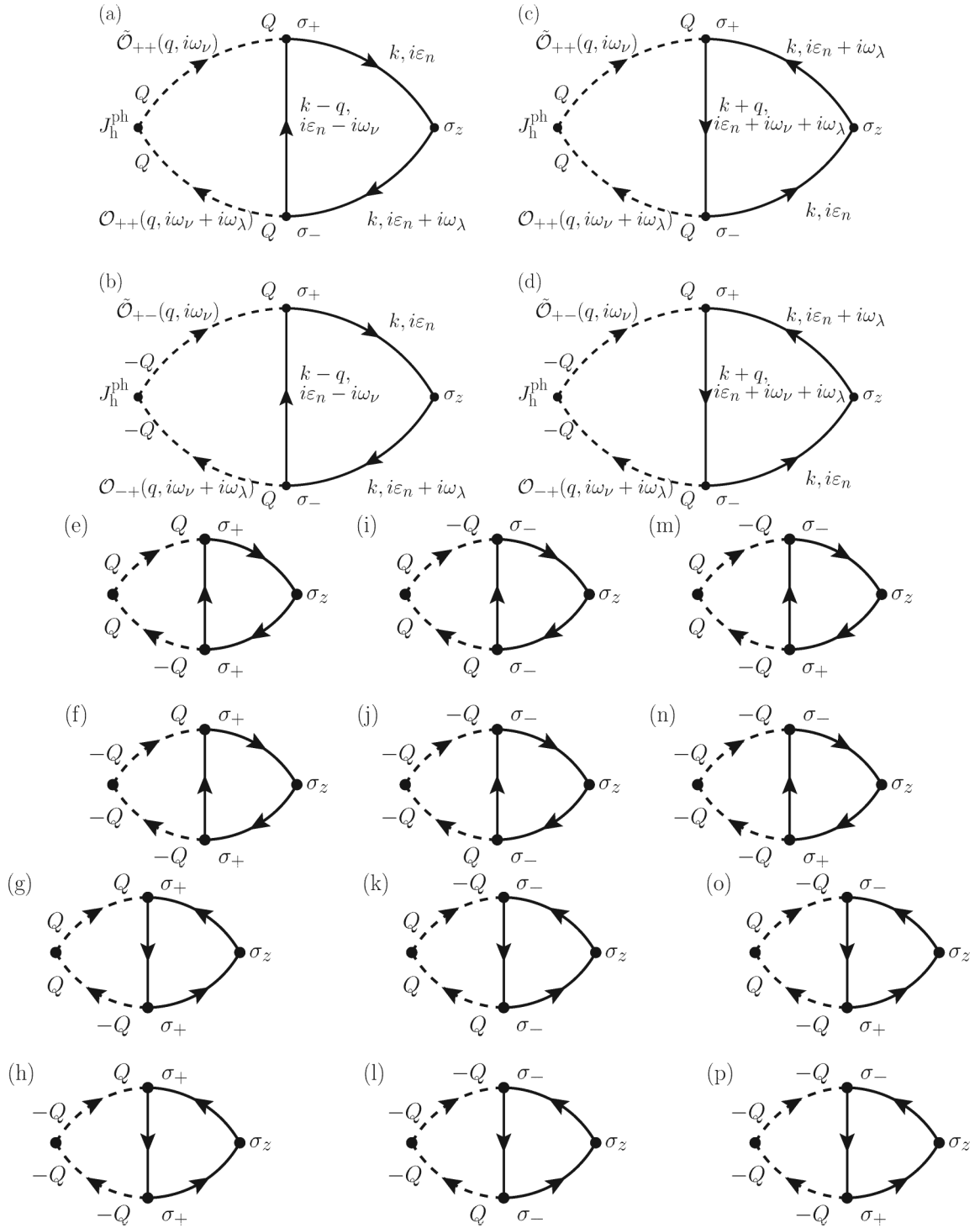
FIG. 4. Feynman diagrams for the phason drag. The solid lines and the dashed lines represent electron and phonon Green's functions, respectively, and the Q and $-Q$ attached to the dashed lines represent the subscripts of the phonon Green's functions O_{mn} and $\tilde{O}_{mn}$, with $m, n = \pm$. (e)–(p) Only the Pauli matrices and the sign of Q are shown, while the momenta and Matsubara frequencies are the same as the corresponding diagrams in (a)–(d).

example, we obtain

Figs. 4(e) + 4(f): $-g_Q^2 \dfrac{(k_B T)^2}{L^2} \displaystyle\sum_{k,q,n,\nu} \hbar\omega_Q c_Q \{ \tilde{O}_{++}(q, i\omega_\nu) O_{+-}(q, i\omega_\nu + i\omega_\lambda) - \tilde{O}_{+-}(q, i\omega_\nu) O_{--}(q, i\omega_\nu + i\omega_\lambda) \}$

$\times e v_F \{ \mathcal{G}_{++}(k, i\varepsilon_n) \mathcal{G}_{-+}(k - q, i\varepsilon_n - i\omega_\nu) \mathcal{G}_{-+}(k, i\varepsilon_n + i\omega_\lambda)$

$- \mathcal{G}_{-+}(k, i\varepsilon_n) \mathcal{G}_{-+}(k - q, i\varepsilon_n - i\omega_\nu) \mathcal{G}_{--}(k, i\varepsilon_n + i\omega_\lambda) \},$

Figs. 4(g) + 4(h) :
$$-g_Q^2 \frac{(k_B T)^2}{L^2} \sum_{k,q,n,\nu} \hbar\omega_Q c_Q \{\tilde{O}_{++}(q, i\omega_\nu)O_{+-}(q, i\omega_\nu + i\omega_\lambda) - \tilde{O}_{+-}(q, i\omega_\nu)O_{--}(q, i\omega_\nu + i\omega_\lambda)\}$$
$$\times ev_F\{\mathcal{G}_{++}(k, i\varepsilon_n)\mathcal{G}_{-+}(k+q, i\varepsilon_n + i\omega_\nu + i\omega_\lambda)\mathcal{G}_{-+}(k, i\varepsilon_n + i\omega_\lambda)$$
$$-\mathcal{G}_{-+}(k, i\varepsilon_n)\mathcal{G}_{-+}(k+q, i\varepsilon_n + i\omega_\nu + i\omega_\lambda)\mathcal{G}_{--}(k, i\varepsilon_n + i\omega_\lambda)\}, \tag{C3}$$

Figs. 4(i) + 4(j):
$$-g_Q^2 \frac{(k_B T)^2}{L^2} \sum_{k,q,n,\nu} \hbar\omega_Q c_Q \{\tilde{O}_{-+}(q, i\omega_\nu)O_{++}(q, i\omega_\nu + i\omega_\lambda) - \tilde{O}_{--}(q, i\omega_\nu)O_{-+}(q, i\omega_\nu + i\omega_\lambda)\}$$
$$\times ev_F\{\mathcal{G}_{+-}(k, i\varepsilon_n)\mathcal{G}_{+-}(k-q, i\varepsilon_n - i\omega_\nu)\mathcal{G}_{++}(k, i\varepsilon_n + i\omega_\lambda)$$
$$-\mathcal{G}_{--}(k, i\varepsilon_n)\mathcal{G}_{+-}(k-q, i\varepsilon_n - i\omega_\nu)\mathcal{G}_{+-}(k, i\varepsilon_n + i\omega_\lambda)\},$$

Figs. 4(k) + 4(l):
$$-g_Q^2 \frac{(k_B T)^2}{L^2} \sum_{k,q,n,\nu} \hbar\omega_Q c_Q \{\tilde{O}_{-+}(q, i\omega_\nu)O_{++}(q, i\omega_\nu + i\omega_\lambda) - \tilde{O}_{--}(q, i\omega_\nu)O_{-+}(q, i\omega_\nu + i\omega_\lambda)\}$$
$$\times ev_F\{\mathcal{G}_{+-}(k, i\varepsilon_n)\mathcal{G}_{+-}(k+q, i\varepsilon_n + i\omega_\nu + i\omega_\lambda)\mathcal{G}_{++}(k, i\varepsilon_n + i\omega_\lambda)$$
$$-\mathcal{G}_{--}(k, i\varepsilon_n)\mathcal{G}_{+-}(k+q, i\varepsilon_n + i\omega_\nu + i\omega_\lambda)\mathcal{G}_{+-}(k, i\varepsilon_n + i\omega_\lambda)\}, \tag{C4}$$

Figs. 4(m) + 4(n):
$$-g_Q^2 \frac{(k_B T)^2}{L^2} \sum_{k,q,n,\nu} \hbar\omega_Q c_Q \{\tilde{O}_{-+}(q, i\omega_\nu)O_{+-}(q, i\omega_\nu + i\omega_\lambda) - \tilde{O}_{--}(q, i\omega_\nu)O_{--}(q, i\omega_\nu + i\omega_\lambda)\}$$
$$\times ev_F\{\mathcal{G}_{+-}(k, i\varepsilon_n)\mathcal{G}_{++}(k-q, i\varepsilon_n - i\omega_\nu)\mathcal{G}_{-+}(k, i\varepsilon_n + i\omega_\lambda)$$
$$-\mathcal{G}_{--}(k, i\varepsilon_n)\mathcal{G}_{++}(k-q, i\varepsilon_n - i\omega_\nu)\mathcal{G}_{--}(k, i\varepsilon_n + i\omega_\lambda)\},$$

Figs. 4(o) + 4(p):
$$-g_Q^2 \frac{(k_B T)^2}{L^2} \sum_{k,q,n,\nu} \hbar\omega_Q c_Q \{\tilde{O}_{-+}(q, i\omega_\nu)O_{+-}(q, i\omega_\nu + i\omega_\lambda) - \tilde{O}_{--}(q, i\omega_\nu)O_{--}(q, i\omega_\nu + i\omega_\lambda)\}$$
$$\times ev_F\{\mathcal{G}_{++}(k, i\varepsilon_n)\mathcal{G}_{--}(k+q, i\varepsilon_n + i\omega_\nu + i\omega_\lambda)\mathcal{G}_{++}(k, i\varepsilon_n + i\omega_\lambda)$$
$$-\mathcal{G}_{-+}(k, i\varepsilon_n)\mathcal{G}_{--}(k+q, i\varepsilon_n + i\omega_\nu + i\omega_\lambda)\mathcal{G}_{+-}(k, i\varepsilon_n + i\omega_\lambda)\}. \tag{C5}$$

The "directed" phonon propagators, O_{mn} and $\tilde{O}_{mn}$, are obtained from the Dyson equations shown in Appendix B. Substituting the explicit form of $\mathcal{G}_{mn}$ in Eq. (9) and using the relationship between O_{mn}, $\tilde{O}_{mn}$, and $\mathcal{D}_{mn}$ obtained in Eq. (B3), the total of Eq. (C1) and Eqs. (C3)–(C5) becomes

$$\Phi_{12}^{ph}(i\omega_\lambda) = -e\hbar v_F \omega_Q c_Q g_Q^2 \frac{(k_B T)^2}{L^2} \sum_{k,q,n,\nu} \frac{i\omega_\nu + \hbar\omega_Q}{2\hbar\omega_Q} \frac{i\omega_\nu + i\omega_\lambda + \hbar\omega_Q}{2\hbar\omega_Q} \frac{2}{(i\varepsilon_n)^2 - E_k^2} \frac{1}{(i\varepsilon_n + i\omega_\lambda)^2 - E_k^2}$$

$$\times \Bigg[\{\mathcal{D}_{++}(q, i\omega_\nu)\mathcal{D}_{++}(q, i\omega_\nu + i\omega_\lambda) - e^{-4i\phi}\mathcal{D}_{+-}(q, i\omega_\nu)\mathcal{D}_{+-}(q, i\omega_\nu + i\omega_\lambda)\}$$

$$\times \{[f(-q, -i\omega_\nu) - f(q, i\omega_\nu + i\omega_\lambda)][i\varepsilon_n(i\varepsilon_n + i\omega_\lambda) + \xi_k^2 - \Delta_0^2]$$

$$- [g(-q, -i\omega_\nu) - g(q, i\omega_\nu + i\omega_\lambda)]\xi_k(2i\varepsilon_n + i\omega_\lambda)\}$$

$$+ \{\mathcal{D}_{++}(q, i\omega_\nu)\mathcal{D}_{+-}(q, i\omega_\nu + i\omega_\lambda) - \mathcal{D}_{+-}(q, i\omega_\nu)\mathcal{D}_{++}(q, i\omega_\nu + i\omega_\lambda)\}$$

$$\times \Bigg\{ -\frac{i\omega_\lambda(\Delta^*)^2}{(i\varepsilon_n - i\omega_\nu)^2 - E_{k-q}^2} - \frac{i\omega_\lambda(\Delta^*)^2}{(i\varepsilon_n + i\omega_\nu + i\omega_\lambda)^2 - E_{k+q}^2} \Bigg\} \Bigg], \tag{C6}$$

where $f(q, i\omega_\nu)$ and $g(q, i\omega_\nu)$ are defined in Eq. (30). The last terms with $i\omega_\lambda(\Delta^*)^2$ can be neglected in the following since it is proportional to $(i\omega_\lambda)^2$. Finally, using the phason and amplitude propagators defined in Eq. (14), we obtain Eq. (29).

APPENDIX D: STRAIGHTFORWARD DERIVATION OF EQUATION (35)

Putting $q = 0$ and $i\omega_\lambda = 0$ in the electron Green's functions in Eq. (C1), the electronic part of $\Phi_{12}^{ph}(i\omega_\lambda)$ corresponding to the diagrams in Figs. 4(a) and 4(c) becomes

$$\sum_k \text{Tr}\big[\mathcal{G}(k, i\varepsilon_n)\sigma_+\mathcal{G}(k, i\varepsilon_n - x)\sigma_-\mathcal{G}(k, i\varepsilon_n)\sigma_z + \mathcal{G}(k, i\varepsilon_n)\sigma_-\mathcal{G}(k, i\varepsilon_n + x)\sigma_+\mathcal{G}(k, i\varepsilon_n)\sigma_z\big], \tag{D1}$$

where $i\omega_\nu$ is replaced by x. To evaluate the trace in Eq. (D1), we use

$$\sigma_+ \begin{pmatrix} a & b \\ c & d \end{pmatrix} \sigma_- = \begin{pmatrix} d & 0 \\ 0 & 0 \end{pmatrix} = \frac{d}{2}(\sigma_0 + \sigma_z),$$

$$\sigma_- \begin{pmatrix} a & b \\ c & d \end{pmatrix} \sigma_+ = \begin{pmatrix} 0 & 0 \\ 0 & a \end{pmatrix} = \frac{a}{2}(\sigma_0 - \sigma_z), \tag{D2}$$

where σ_0 is the 2×2 unit matrix. When $x = 0$, the trace in Eq. (D1) becomes

$$\frac{1}{2}\mathrm{Tr}\Big[\mathcal{G}(k, i\varepsilon_n)\frac{i\varepsilon_n - \xi_k}{(i\varepsilon_n)^2 - E_k^2}(\sigma_0 + \sigma_z)\mathcal{G}(k, i\varepsilon_n)\sigma_z + \mathcal{G}(k, i\varepsilon_n)\frac{i\varepsilon_n + \xi_k}{(i\varepsilon_n)^2 - E_k^2}(\sigma_0 - \sigma_z)\mathcal{G}(k, i\varepsilon_n)\sigma_z\Big]$$

$$= \frac{1}{(i\varepsilon_n)^2 - E_k^2}\mathrm{Tr}[\mathcal{G}(k, i\varepsilon_n)(i\varepsilon_n\sigma_0 - \xi_k\sigma_z)\mathcal{G}(k, i\varepsilon_n)\sigma_z]$$

$$= \frac{2}{[(i\varepsilon_n)^2 - E_k^2]^3}\big[i\varepsilon_n \times (2i\varepsilon_n\xi_k) - \xi_k \times \big((i\varepsilon_n)^2 + \xi_k^2 - \Delta_0^2\big)\big]. \tag{D3}$$

This vanishes since the last expression is odd with respect to k. The lowest order with respect to x becomes, in a similar way,

$$x\,\mathrm{Tr}[\mathcal{G}(k, i\varepsilon_n)\sigma_+\mathcal{G}^2(k, i\varepsilon_n)\sigma_-\mathcal{G}(k, i\varepsilon_n)\sigma_z - \mathcal{G}(k, i\varepsilon_n)\sigma_-\mathcal{G}^2(k, i\varepsilon_n)\sigma_+\mathcal{G}(k, i\varepsilon_n)\sigma_z],$$

$$= \frac{x}{\big[(i\varepsilon_n)^2 - E_k^2\big]^2}\mathrm{Tr}\big[\mathcal{G}(k, i\varepsilon_n)\big\{-2i\varepsilon_n\xi_k\sigma_0 + \big[(i\varepsilon_n)^2 + \xi_k^2 + \Delta_0^2\big]\sigma_z\big\}\mathcal{G}(k, i\varepsilon_n)\sigma_z\big]$$

$$= \frac{2x}{\big[(i\varepsilon_n)^2 - E_k^2\big]^4}\big\{-2i\varepsilon_n\xi_k \times (2i\varepsilon_n\xi_k) + \big[(i\varepsilon_n)^2 + \xi_k^2 + \Delta_0^2\big] \times \big[(i\varepsilon_n)^2 + \xi_k^2 - \Delta_0^2\big]\big\}$$

$$= \frac{2x}{\big[(i\varepsilon_n)^2 - E_k^2\big]^4}\big\{\big[(i\varepsilon_n)^2 - \xi_k^2\big]^2 - \Delta_0^4\big\}, \tag{D4}$$

which leads to Eq. (35). Other contributions in Fig. 4 are treated similarly.

APPENDIX E: CALCULATION OF $D(T)$

$$D(T) = -\frac{k_B T}{L}\sum_{k,n}\frac{(i\varepsilon_n)^2 - \xi_k^2 + \Delta_0^2}{\big[(i\varepsilon_n)^2 - E_k^2\big]^3}$$

$$= \frac{1}{L}\sum_k \oint \frac{dz}{2\pi i}f(z)\Big[\frac{1}{(z^2 - E_k^2)^2} + \frac{2\Delta_0^2}{(z^2 - E_k^2)^3}\Big]$$

$$= -\frac{1}{L}\sum_k \sum_\pm \Big[\pm\frac{\Delta_0^2 f''(\pm E_k)}{8E_k^3} + \frac{2E_k^2 - 3\Delta_0^2}{8E_k^4}f'(\pm E_k)$$

$$\mp \frac{2E_k^2 - 3\Delta_0^2}{8E_k^5}f(\pm E_k)\Big], \tag{E1}$$

where $f(\varepsilon) = 1/(e^{\beta\varepsilon} + 1)$, i.e., the Fermi distribution function with $\mu = 0$. At $T = 0$, we have

$$D(0) = -\frac{1}{L}\sum_k \frac{2E_k^2 - 3\Delta_0^2}{8E_k^5}. \tag{E2}$$

Using the relation

$$\frac{d}{dk}\Big(\frac{k}{E_k^3}\Big) = -\frac{2E_k^2 - 3\Delta_0^2}{E_k^5}, \tag{E3}$$

Eq. (E2) becomes

$$D(0) = \frac{k_F}{8\pi E_{k_F}^3}, \tag{E4}$$

where we set the range of k as $|k| < k_F$, as assumed in Eq. (3).

APPENDIX F: PHASE HAMILTONIAN AND PHASON PROPAGATOR

The phason propagator (38) at $T = 0$ is derived from previous studies based on the phase Hamiltonian approach. The model of a phason coupled to randomly distributed impurities is given by [18,19]

$$H_0 = \pi\hbar v'\int dx\Big[p^2 + \frac{1}{4\pi^2}\Big(\frac{v}{v'}\Big)^2(\nabla\phi)^2\Big] \tag{F1}$$

and

$$H' = V_0\rho_0\sum_i \cos[QR_i + \phi(R_i)], \tag{F2}$$

where v is the phason velocity given in Eq. (16) and $v' = v^2/|v_F|$. The first one is the field theory for the phase variable $\phi(x)$, while the second represents the coupling to impurities of CDW expressed in terms of $\phi(x)$, which is derived from the impurity Hamiltonian H' in Eq. (1) and the charge density $\rho(x)$ in Eq. (6), assuming that $v(r - R_i) = V_0\delta(x - R_i)$. The electrical conductivity for a uniform electric field with finite frequency ω, $\sigma(\omega)$, is given as follows by noting that the current density operator is represented as $-(e/\pi)\partial\phi(x, t)/\partial t$ [14,18]:

$$\sigma(\omega) = -\frac{i\omega}{2}\Big(\frac{e}{\pi}\Big)^2 L\mathcal{D}(0, 0; i\omega_n)\big|_{i\omega_n \to \hbar\omega + i\delta}, \tag{F3}$$
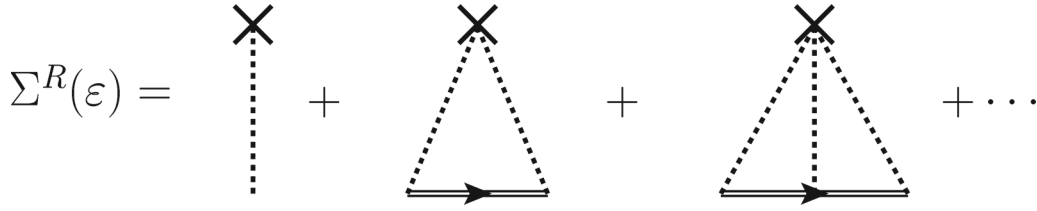
FIG. 5. Feynman diagrams in the t-matrix approximation. Crosses represent the impurity potential, and the solid double lines show the phason propagator.

where the phason Green's function is defined by

$$\mathcal{D}(q, q'; i\omega_n) = 2 \int_0^\beta d\tau e^{i\omega_n \tau} \langle T_\tau [\phi_q(\tau) \phi_{-q'}(0)] \rangle \quad \text{(F4)}$$

and ϕ_q is the Fourier transform of $\phi(x)$, defined as

$$\phi_q = \frac{1}{L} \int dx e^{-iqx} \phi(x). \quad \text{(F5)}$$

It should be noted that the formulation in [18,19], in particular the convention of ω, is changed in accordance with the present framework.

Here, we note that the phonon operator $b_{Q+q}(\tau) + b_{-Q-q}^\dagger(\tau)$ can be expressed in terms of the phase and amplitude variables as

$$b_{Q+q}(\tau) + b_{-Q-q}^\dagger(\tau) \sim \frac{\sqrt{L}}{g_Q} [\Delta_0 + \delta\Delta_q(\tau)] e^{i[\phi + \delta\phi_q(\tau)]}, \quad \text{(F6)}$$

where $\delta\Delta_q(\tau)$ represents the modulation of the amplitude and $\delta\phi_q(\tau)$ represents the deviation from the constant ϕ. Substituting this expression into the phonon propagator in Eq. (7) and using the expansion $e^{i\delta\phi_q(\tau)} \sim 1 + i\delta\phi_q(\tau)$, we obtain

$$\mathcal{D}_{++}(q, \tau) \sim -\frac{L}{g_Q^2} \langle T_\tau [\delta\Delta_q(\tau) \delta\Delta_{-q}(0)] \rangle$$
$$- \frac{L\Delta_0^2}{g_Q^2} \langle T_\tau [\delta\phi_q(\tau) \delta\phi_{-q}(0)] \rangle,$$

$$\mathcal{D}_{+-}(q, \tau) \sim -\frac{L}{g_Q^2} e^{2i\phi} \langle T_\tau [\delta\Delta_q(\tau) \delta\Delta_{-q}(0)] \rangle$$
$$+ \frac{L\Delta_0^2}{g_Q^2} e^{2i\phi} \langle T_\tau [\delta\phi_q(\tau) \delta\phi_{-q}(0)] \rangle. \quad \text{(F7)}$$

Hence, we obtain, by noting $\phi_q = \phi + \delta\phi_q$,

$$P(q, i\omega_n) = \mathcal{D}_{++}(q, i\omega_n) - e^{-2i\phi} \mathcal{D}_{+-}(q, i\omega_n)$$
$$= -2\frac{L\Delta_0^2}{g_Q^2} \int_0^\beta d\tau e^{i\omega_n \tau} \langle T_\tau [\delta\phi_q(\tau) \delta\phi_{-q}(0)] \rangle$$
$$= -\frac{L\Delta_0^2}{g_Q^2} \mathcal{D}(q, i\omega_n), \quad \text{(F8)}$$

which proves the equivalence between Eqs. (24) and (F3).

In a clean system without disorder this phason propagator governed by (F1) is given by $\mathcal{D}(q, q'; i\omega_n) = \delta_{q,q'} \mathcal{D}_0(q, i\omega_n)$, with

$$\mathcal{D}_0(q, i\omega_n) = \frac{1}{L} \frac{4\pi\hbar v'}{\omega_n^2 + \hbar^2 v^2 q^2}. \quad \text{(F9)}$$

By noting $v = (m/m^*)^{1/2} |v_F|$, with m^* being the effective mass of the phason mode $\sigma(\omega)$, Eq. (F3), in this case for spatially uniform electric field ($q = 0$), is

$$\sigma(\omega) = \frac{in_e e^2}{m^* \omega}, \quad \text{(F10)}$$

which is the same as that of LRA. Equation (F10) is considered to be a manifestation of Fröhlich superconductivity in the Peierls phase without disorder.

The effects of impurity scattering on the phason propagator are given by the self-energy correction Γ, defined by

$$\langle \mathcal{D}(q, q'; i\omega_n) \rangle_{av} = \delta_{q+q'} [\mathcal{D}_0(q)^{-1} - \Gamma]^{-1} = \delta_{q+q'} \mathcal{D}(q, i\omega_n). \quad \text{(F11)}$$

The t-matrix approximation to Γ is given by the processes in Fig. 5. As clarified in Ref. [19], the effects of impurity pinning can be classified typically into weak and strong, characterized by the parameter $\varepsilon = V_0 \rho_0 / n_i \hbar |v_F|$. We focus on the case of weak pinning, $\varepsilon \ll 1$, for generality. In this case, the first- and second-order terms in Fig. 5 are sufficient. The first-order contribution is given by

$$\Gamma_1 = \frac{V_0 \rho_0}{2L} \sum_i \cos[QR_i + \phi(R_i)]. \quad \text{(F12)}$$

This contribution is vanishing if the phase is rigid, i.e., spatially constant. However, there is a gain in energy due to spatial distortions of ϕ, reflecting the distribution of impurities leading to domains with characteristic size L_0, which is given by (similar to a random walk problem)

$$\Gamma_1 = -\frac{1}{2} V_0 \rho_0 (n_i L_0)^{1/2} / L_0. \quad \text{(F13)}$$

Here, the size L_0 should be determined by optimizing the energy gain (F13) against the energy loss due to the spatial distortion of the phase represented by the second term of (F1), leading to $(n_i L_0)^{-1} = (\alpha \pi \varepsilon)^{2/3}$, where the parameter α reflects the way of the phase distortion of the order of π. The study in [19] has indicated that $\alpha = 3^3/2^5$ is the best choice. This is the essence of impurity pinning. The second-order contribution is given by

$$\Gamma_2 = \left(\frac{V_0 \rho_0}{2L}\right)^2 \sum_{q \neq 0} \mathcal{D}(q, \hbar\omega) \sum_{i,j} e^{iq(R_i - R_j)} \cos[QR_i + \phi(R_i)]$$
$$\times \cos[QR_j + \phi(R_j)]$$
$$= \frac{n_i}{2} \left(\frac{V_0 \rho_0}{2}\right)^2 2\pi \frac{v'}{v} (-\hbar^2 \omega^2 - 4\pi\hbar v' \Gamma)^{-1/2}. \quad \text{(F14)}$$

The self-consistent equation for $\Gamma = \Gamma_1 + \Gamma_2$ given by (F13) and (F14) leads to

$$G = -2\alpha^{1/3} + (-y^2 - G)^{-1/2}, \qquad \text{(F15)}$$

where $G = 4\pi\hbar v'\Gamma/\gamma^2$ and $y = \hbar\omega/\gamma$, with $\gamma = (\pi\varepsilon)^{2/3}\omega_0$ and $\omega_0 = n_i\hbar v$. For low frequency, $y < 1$, the solution of the self-consistent equation for G with the proper choice of parameter characterizing the effects of impurity scattering for causality to be satisfied is found to be $G \sim -a_0 + ia_1 y$, with

$a_0 = 1/2^{2/3} = 0.630$ and $a_1 = (2^{4/3}/3)^{1/2} = 0.916$, which leads to

$$\mathcal{D}(q, \hbar\omega + i\delta) = \frac{1}{L} \frac{4\pi\hbar v'}{-(\hbar\omega + i\delta)^2 + \hbar^2 v^2 q^2 + g_0 - i\hbar\omega g_1}, \qquad \text{(F16)}$$

where $g_0 = \gamma^2 a_0$ and $g_1 = \gamma a_1$. Equations (F16) and (F8), together with $v' = v^2/|v_F|$, $v = [X/(1+X)]^{1/2}|v_F|$, and $X = \omega_Q g_Q^2/2\pi|v_F|\Delta_0^2$, lead to (38).

---

[1] For a review, see G. D. Mahan, Good thermoelectrics, Solid State Phys. **51**, 81 (1997).

[2] K. Behnia, *Fundamentals of Thermoelectricity* (Oxford University Press, Oxford, 2015).

[3] R. Kubo, Statistical-mechanical theory of irreversible processes. I. General theory and simple applications to magnetic and conduction problems, J. Phys. Soc. Jpn. **12**, 570 (1957).

[4] J. M. Luttinger, Theory of thermal transport coefficients, Phys. Rev. **135**, A1505 (1964).

[5] M. Ogata and H. Fukuyama, Theory of spin Seebeck effects in a quantum wire, J. Phys. Soc. Jpn. **86**, 094703 (2017).

[6] M. Ogata and H. Fukuyama, Range of validity of Sommerfeld-Bethe relation associated with Seebeck coefficient and phonon drag contribution, J. Phys. Soc. Jpn. **88**, 074703 (2019).

[7] H. Matsuura, H. Maebashi, M. Ogata, and H. Fukuyama, Effect of phonon drag on Seebeck coefficient based on linear response theory: Application to FeSb$_2$, J. Phys. Soc. Jpn. **88**, 074601 (2019).

[8] T. Yamamoto and H. Fukuyama, Possible high thermoelectric power in semiconducting carbon nanotubes—a case study of doped one-dimensional semiconductors, J. Phys. Soc. Jpn. **87**, 024707 (2018).

[9] T. Yamamoto and H. Fukuyama, Bipolar thermoelectric effects in semiconducting carbon nanotubes: Description in terms of one-dimensional dirac electrons, J. Phys. Soc. Jpn. **87**, 114710 (2018).

[10] L. Gurevich, Thermoelectric properties of conductors. I, J. Phys. (Moscow) **9**, 477 (1945).

[11] C. Herring, Theory of the thermoelectric power of semiconductors, Phys. Rev. **96**, 1163 (1954).

[12] G. D. Mahan, L. Lindsay, and D. A. Broido, The Seebeck coefficient and phonon drag in silicon, J. Appl. Phys. **116**, 245102 (2014).

[13] J. Zhou, B. Liao, B. Qiu, S. Huberman, K. Esfarjani, M. S. Dresselhaus, and G. Chen, Ab initio optimization of phonon drag effect for lower-temperature thermoelectric energy conversion, Proc. Natl. Acad. Sci. **112**, 14777 (2015).

[14] P. A. Lee, T. M. Rice, and P. W. Anderson, Conductivity from charge or spin density waves, Solid State Commun. **14**, 703 (1974).

[15] L. B. Coleman, M. J. Cohen, D. J. Sandman, F. G. Yamagishi, A. F. Garito, and A. J. Heeger, Superconducting fluctuations and the Peierls instability in an organic solid, Solid State Commun. **12**, 1125 (1973).

[16] M. J. Cohen, L. B. Coleman, A. F. Garito, and A. J. Heeger, Electrical conductivity of tetrathiofulvalinium tetracyanoquinodimethan (TTF) (TCNQ), Phys. Rev. B **10**, 1298 (1974).

[17] H. Yoshimoto and S. Kurihara, Thermal transport properties of a charge density wave, J. Phys. Soc. Jpn. **75**, 014601 (2006).

[18] H. Fukuyama, Pinning in peierls-Fröhlich state and conductivity, J. Phys. Soc. Jpn. **41**, 513 (1976).

[19] H. Fukuyama and P. A. Lee, Dynamics of the charge-density wave. I. Impurity pinning in a single chain, Phys. Rev. B **17**, 535 (1978).

[20] H. Fukuyama and H. Takayama, *Electronic Properties of Inorganic Quasi-One-Dimensional Materials*, edited by P. Monceau (Reidel, Dordrecht, Boston, London, 1985).

[21] K. Baumann, Quantum theory of transport coefficients. II, Ann. Phys. (NY) **23**, 221 (1963).

[22] Similar processes were considered in the following study on the magnon drag phenomena: D. Miura and A. Sakuma, Microscopic theory of magnon-drag thermoelectric transport in ferromagnetic metals, J. Phys. Soc. Jpn. **81**, 113602 (2012).

[23] N. Okuma and K. Nomura, Microscopic derivation of magnon spin current in a topological insulator/ferromagnet heterostructure, Phys. Rev. B **95**, 115403 (2017).

[24] T. Yamaguchi and H. Kohno, Microscopic theory of spin-wave spin torques induced by temperature gradient, J. Phys. Soc. Jpn. **86**, 063706 (2017).

[25] Y. Imai and H. Kohno, Theory of cross-correlated electron-magnon transport phenomena: Case of magnetic topological insulator, J. Phys. Soc. Jpn. **87**, 073709 (2018).

[26] M. Baggioli and A. Zaccone, Universal Origin of Boson Peak Vibrational Anomalies in Ordered Crystals and in Amorphous Materials, Phys. Rev. Lett. **122**, 145501 (2019).

[27] P. W. Anderson, P. A. Lee, and M. Saitoh, Remarks on giant conductivity in TTF-TCNQ, Solid State Commun. **13**, 595 (1973).

[28] H. Fukuyama, Commensurability pinning versus impurity pinning of one-dimensional charge density wave, J. Phys. Soc. Jpn. **45**, 1474 (1978).

[29] H. Fukuyama, J. Kishine, and M. Ogata, Energy landscape of charge excitations in the boundary region between dimer-mott and charge ordered states in molecular solids, J. Phys. Soc. Jpn. **86**, 123706 (2017).

[30] J. F. Kwak, P. M. Chaikin, A. A. Russel, A. F. Garito, and A. J. Heeger, Anisotropic thermoelectric power of TTF-TCNQ, Solid State Commun. **16**, 729 (1975).